Journal of Membrane Science 510 (2016) 466–471

Contents lists available at ScienceDirect

Journal of Membrane Science

journal homepage: www.elsevier.com/locate/memsci

Toward gas-phase controlled mass transfer in micro-porous membrane contactors for recovery and concentration of dissolved methane in the gas phase

Andrew McLeod, Bruce Jefferson, Ewan J. McAdam *

Cranfield Water Science Institute, Cranfield University, Vincent Building (52a), Bedfordshire, MK43 0AL, UK

ARTICLE INFO

Article history:
Received 22 December 2015
Received in revised form
11 March 2016
Accepted 15 March 2016
Available online 18 March 2016

Keywords:
Dissolved methane recovery
Degas
Degassing
Anaerobic
Landfill leachate

ABSTRACT

A micro-porous hollow fibre membrane contactor (HFMC) operated in sweep-gas mode has been studied to enable the recovery of dissolved methane from water in concentrated form. At high sweep-gas flow rates, up to 97% dissolved methane removal efficiency is achievable which is sufficient to achieve carbon neutrality (around 88%). An increase in methane composition of the recovered sweep-gas was achievable through two primary mechanisms: (i) an increase in liquid velocity which improved dissolved methane mass transfer into the gas phase; and (ii) a reduction in gas flow which lowered dilution from the receiving gas phase. It was posited that further refinement of the methane content was provided through counter-diffusion of the nitrogen sweep-gas into the liquid phase. Within the boundary conditions studied, the methane composition of the recovered gas phase exceeded the threshold for use in micro-turbines for electricity production. However, reducing the gas-to-liquid ratio to enhance gas phase methane purity introduced gas-phase controlled mass transfer which constrained removal efficiency. Whilst this reduction in removal efficiency can be compensated for by extending path length (i.e. more than one module in series), it is suggested that the gas-phase controlled conditions encountered were also a product of poor shell-side dispersion rather than an approach toward the limiting theoretical gas-to-liquid ratio. This implies that further optimisation can be ascertained through improved membrane contactor design. Importantly, this study demonstrates that micro-porous hollow fibre membrane contactors provide a compact process for recovery of dissolved methane in sufficient concentration for re-use.

1. Introduction

Methane (CH_4) generated from engineered anaerobic environments, such as landfills or anaerobic wastewater treatment systems, can be used in combustion for the production of electricity. However, the effluent produced from these systems is typically at equilibrium with the gas phase which is often characterised by a high CH_4 partial pressure (50–75%) and results in production of anaerobic effluent rich in dissolved methane.

Multi-stage bubble column cross-flow cascades are often used for dissolved methane separation from contaminated water (e.g. for the treatment of landfill leachate), in which the bubble column provides contact between the dissolved methane laden anaerobic effluent and a 'sweep gas'. The driving force for separation is provided by the sweep gas which introduces a concentration gradient at the gas-liquid interface [1]. High gas-to-liquid ratios of 10:1–15:1 are typically employed to ensure that the air phase does not restrict mass transfer and that the off-gas phase is well below the lower explosion limit for methane (around 5% v/v), which subsequently yields an off-gas methane concentration of less than 0.028% [2]. Whilst this is satisfactory for safe direct venting of the separated methane to atmosphere, this is substantially below the gas phase methane concentration of around 35% v/v that is required if the recovered methane is to be reused for conversion to electricity [3]. Cookney et al. (2012) identified that over 50% of the methane produced during the anaerobic treatment of municipal wastewater was dissolved in the reactor effluent thus the recovery of dissolved methane in sufficient concentration for reuse is critical to enhancing overall energy production capacity from anaerobic wastewater treatment and to diminish the respective carbon footprint through limiting the fugitive release of methane [4], which is 21 times more potent than carbon dioxide (CO_2) as a greenhouse gas (GHG) [5,6].

In principle, the high volatility of methane ($H_{dimensionless}$, 28.41) indicates that a considerably lower G/L ratio, than previously used in bubble columns, can be employed for the separation of

* Corresponding author.
E-mail address: e.mcadam@cranfield.ac.uk (E.J. McAdam).

http://dx.doi.org/10.1016/j.memsci.2016.03.030

dissolved methane from wastewater [7]:

$$\left(\frac{Q_G}{Q_L}\right)_{minimum} = \frac{c_{in} - c_{out}}{Hc_{in}} \quad (1)$$

where Q_G and Q_L are sweep-gas and liquid flow rates, c_{in} and c_{out} are the inlet and outlet liquid phase concentrations and H is the dimensionless Henry's constant. To illustrate, the theoretical minimum gas-to-liquid ratio required to achieve 90% dissolved methane removal is G/L 0.032, suggesting an achievable methane concentration of 47% in the sweep gas, which is above the threshold required for conversion to electricity. However, it is generally recognised that a G/L ratio 3.5 times higher than the minimum G/L is required in bubble column aerators to avoid gas phase controlled operation which can restrict mass transfer [8].

Hollow fibre membrane contactor (HFMC) technology promotes the same desorption mechanism to bubble column aerators. However, the hydrophobic micro-porous membrane facilitates non-dispersive contact between the liquid and gas phases, enabling the methane to diffuse through the gas filled pores [9]. Consequently, similar removal efficiencies to bubble column aerators have been observed with HFMC but at considerably lower gas-to-liquid ratios [10] therefore providing a potential route to enhancing the methane concentration in the recovered gas phase. Whilst this specific advantage over conventional technology has been characterised, very few studies to date have focussed on concentrating the stripped solute within the recovered gas phase. Cramer et al. first studied the application of hollow fibre membranes for dissolved methane separation as an in-situ method for methane recovery from a coal seam [11]. Through semi-empirical modelling, the authors estimated that a gas phase concentration of up to 97% CH_4 was achievable when dissolved methane was saturated at a pressure of 1.05×10^3 kPa which is markedly above the partial pressures observed in typical environmental applications. Bandara et al. employed vacuum instead of sweep gas as the driving force when studying the application of a non-porous polyethylene composite hollow fibre membrane for the recovery of dissolved methane from the effluent of an anaerobic reactor treating low strength wastewater [12]. A CH_4 composition in the gas phase of around 20% was identified although it was asserted that CH_4 composition was underestimated due to air ingress into the dissolved gas collection line. Whilst their study importantly demonstrated the potential for dissolved methane recovery, the use of non-porous membranes is known to limit mass transfer [1,9] necessitating residence times for degassing of up to 9.2 h which are practically constraining [12]. In this study, a commercially available hydrophobic micro-porous hollow fibre membrane contactor is therefore used which has been shown to enable dissolved methane recovery within residence times of 1.5–12.5 s [1]. Vacuum can also be applied as the driving force for degassing with micro-porous HFMC, however, the necessary vacuum pressures can promote pore wetting which noticeably reduces gas transport across the micro-pores and hence diminishes mass transfer [13]. Consequently, in this study, sweep-gas is used to provide the driving force. This therefore represents the first examination of sweep-gas to recover dissolved methane at sufficient concentration in the gas phase for use in the production of renewable energy. Specific objectives are to: (i) determine the limiting effect of a reduction in gas-to-liquid ratio on dissolved methane removal efficiency; (ii) determine the hydrodynamic boundary conditions that govern methane concentration in the gas phase; and (iii) establish whether gas side methane purity (sufficient for reuse) is practicably attainable.

2. Materials and methods

2.1. Equipment setup and operation

A 10 L volume of de-ionised (DI) water (15 MΩ cm^{-1}) was maintained at 25 °C in a water bath with a thermostatic circulator (GD120, Grant Instruments Cambridge Ltd., UK). A CH_4/CO_2 (75:25) gas mixture was passed through the liquid at a flow rate of 1.7×10^{-5} m^3 s^{-1} for one hour, which was determined as sufficient to achieve saturation. Gas flow was continued throughout each experiment to maintain saturation. Gases (CH_4, 99.995% and CO_2, 99.7%, BOC gases, UK) were independently controlled and monitored by mass flow controllers (MFC, 0.2–20 L min^{-1}, Roxspur Measurement and Control Ltd., UK) and mixed in line (Fig. 1). Based upon a Henry's constant of 0.0015 mol L^{-1} atm^{-1} determined for CH_4 at 25 °C and a partial pressure of 0.75 atm CH_4, the estimated initial CH_4 concentration ($c_{CH4,\ in}$) in the liquid phase was 18 mg_{CH4} L^{-1} [14,15] which was confirmed through subsequent analysis.

Upon saturation the liquid was fed to the lumen-side of the HFMC (Liqui-Cel® 1.7 × 5.5 MiniModule®, Membrana GmbH, Germany) using a peristaltic pump (520, Watson-Marlow Pumps,

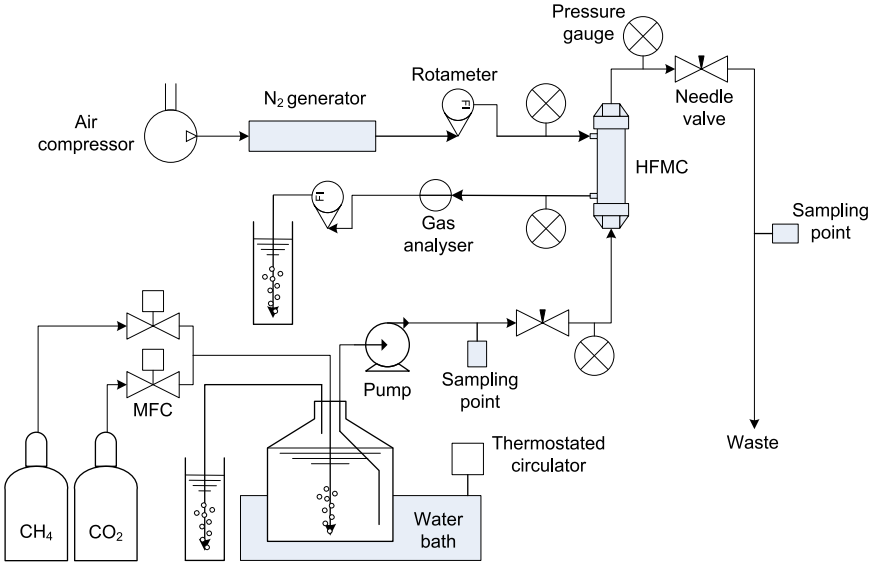

Fig. 1. Schematic of the membrane degas apparatus, including liquid saturation aspirator, sweep gas generation equipment and degassing membrane module (HFMC).

UK). The HFMC comprised 7400 polypropylene (PP) fibres possessing nominal inner diameters (ID) of 220 μm, outer diameters (OD) of 300 μm, a mean pore size of 0.03 μm and 40% porosity. An active length of 0.113 m was determined from the total surface area of 0.58 m^2 given by the manufacturer based on the fibre ID. Fibres were potted in polyurethane within a polycarbonate shell, with a diameter of 0.0425 m, resulting in an average packing fraction (θ) of 0.369. N_2 sweep gas was produced from compressed air using a nitrogen generator that was then regulated to below 1 bar(g) and fed through the HFMC shell counter-currently to the liquid. Sweep gas flow rate was controlled using a needle valve and measured before and after the HFMC by a variable area flow metre (Key Instruments, USA).

2.2. Sampling and analysis

Luer lock fittings were installed in the liquid line upstream and downstream of the HFMC to enable direct liquid sample collection without sample exposure to atmosphere. Samples were collected in evacuated vials (Vacutainer, Becton Dickinson and Company, USA). The reduced pressure in the vials allowed collection of the liquid samples, leaving a small headspace above the liquid upon equilibration to atmospheric pressure. Liquid samples were agitated for 7 minutes (maximum speed, Multi Reax, Heidolph, Germany), and left to equilibrate overnight. The resultant dissolved phase concentrations were calculated based on the modified method of Alberto et al. (2000) [16]. Headspace gas samples were analysed using a gas chromatograph fitted with a thermal conductivity detector (200 Series, Cambridge Scientific Instruments Ltd., UK). The GC-TCD was also used to confirm accuracy of the CH_4 and CO_2 mass flow controller's factory calibrations. Calibration of the GC-TCD was undertaken using certified gas standards (Scientific Technical Gases Ltd., UK) prior to each analysis, where the lowest standard (1% CH_4) represented the effective limit of detection. Methane contained within the sweep-gas was measured using an in-line infra-red biogas analyser sited downstream of the HFMC (Yieldmaster, Bluesens gas sensor GmbH, Herten, Germany). The recorded value represented an average of 5 consecutive data points; the measurement range was 0–100% volume CH_4 with an accuracy of 0.2% of full scale.

2.3. Mass transfer and minimum G/L calculations

The liquid phase mass transfer coefficient was determined using [17]:

$$k_L = \frac{-Q_L}{(\pi d L n)}\left[\frac{1}{\left(1-\frac{Q_L}{Q_G H}\right)}\right]\times \ln\left[\frac{c_{CH_4,in}}{\left(1-\frac{Q_L}{Q_G H}\right)c_{CH_4,in}+\left(\frac{Q_L}{Q_G H}\right)c_{CH_4,out}}\right] \quad (2)$$

where k_L is the mass transfer coefficient (m s^{-1}), d is the single membrane fibre ID, n is the number of fibres, L is the active length, $c_{CH4,\ in}$ and $c_{CH4,\ out}$ are the dissolved methane concentrations in and out of the HFMC respectively (mg m^{-3}), Q_L and Q_G are liquid and gas flow rates respectively (m^3 s^{-1}) and H is the dimensionless Henry's constant. As liquid was processed on the lumen-side, the Graetz–Lévèque solution was employed to estimate Sherwood number (Sh) [18]:

$$Sh = \frac{k_L d}{D} = 1.62\left(\frac{d^2 V_L}{DL}\right)^{0.33} = 1.62 Gz^{0.33} \quad (3)$$

where d is characteristic length (equivalent to a single membrane fibre ID, m), D is the CH_4 gas diffusion coefficient (D 1.88×10^{-9} m^2 s^{-1}) [15], V_L is liquid velocity (m s^{-1}) and Gz is the dimensionless Graetz number. Reynolds number (Re) of the fluid (either the liquid or gas phase) was determined by:

$$Re = \frac{\rho d V}{\mu} \quad (4)$$

where ρ is the fluid density (kg m^{-3}), V is the fluid velocity (m s^{-1}) and μ is the dynamic viscosity of the fluid (kg m^{-1} s^{-1}). The characteristic length (d, m) was provided by the hollow fibre inner diameter for water transport in the lumen-side, whereas for shell-side transport, the wetted perimeter was used [18].

3. Results

3.1. Dissolved methane removal efficiency

Dissolved methane removal efficiency exceeded 90% at the lower liquid flow rates (Q_L) of the Q_L range tested, when sweep gas flow rates (Q_G) were fixed to between 1.7×10^{-4} and 1.7×10^{-6} m^3 s^{-1} (Fig. 2). However, as liquid flow rate was increased above around 0.25×10^{-5} m^3 s^{-1}, dissolved methane removal efficiency declined to between 50% and 60%. Comparison of removal efficiency data at each of the fixed Q_G evaluated demonstrated that as Q_G was lowered, a reduction in dissolved methane removal efficiency was observed. This reduction in removal efficiency was exacerbated at Q_G 1.7×10^{-7} m^3 s^{-1} which was the lowest Q_G evaluated. To illustrate, at Q_G 1.7×10^{-7} m^3 s^{-1}, a maximum removal efficiency of 21% was recorded which reduced to just 3% as Q_L was increased to a maximum of 1.2×10^{-5} m^3 s^{-1}.

Dissolved methane removal efficiency data was re-evaluated to enable comparison to the minimum theoretical gas to liquid (G/L) ratio that is required to achieve the specified dissolved methane removal efficiency (Fig. 3). Maximum removal efficiency (97%) was achieved at a G/L of 200 (Q_G, 1.7×10^{-4} m^3 s^{-1}; Re_{gas}= 77,700), which is over 6000 times higher than the corresponding theoretical minimum G/L (0.033). Similarly, analogous removal efficiency (97%) was achieved at a much lower G/L of 15.6 (Q_G 1.7×10^{-5} m^3 s^{-1}, Re_{gas}=7770) at an approximately constant Q_L (1×10^{-6} m^3 s^{-1}, Re_{liquid}=1). However, whilst each Q_G examined provides hydrodynamic conditions that broadly exceed the theoretical minimum G/L ratio, dissolved methane removal efficiency declined at each gas flow rate as the G/L ratio tended closer toward the minimum. For example, at a fixed Q_G of 1.7×10^{-6} m^3 s^{-1}, dissolved methane removal efficiency declined from 86% to 66% as G/L was reduced from 0.5 to 0.25.

3.2. Dissolved methane mass transfer analysis

Experimental data was characterised in the dimensionless form of the Sherwood number (Eq. (2)) to represent the ratio of the rate

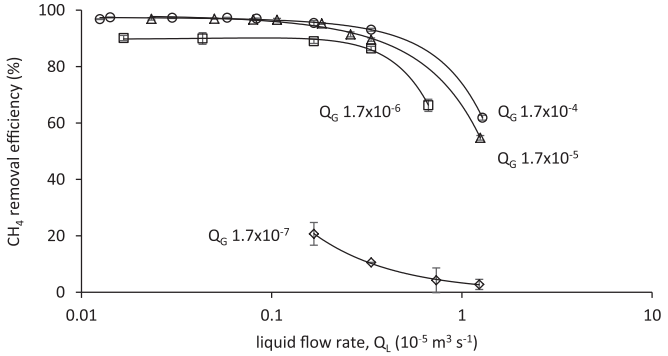

Fig. 2. CH_4 removal efficiencies from water saturated by a CH_4/CO_2 mixture (75/25, 1 atm, 25 °C) for different magnitudes of sweep-gas Q_G ($1.7\times10^{-7}-1.7\times10^{-4}$ m^3 s^{-1}) against variable Q_L ($1.3\times10^{-7}-1.3\times10^{-5}$ m^3 s^{-1}) using a HFMC.

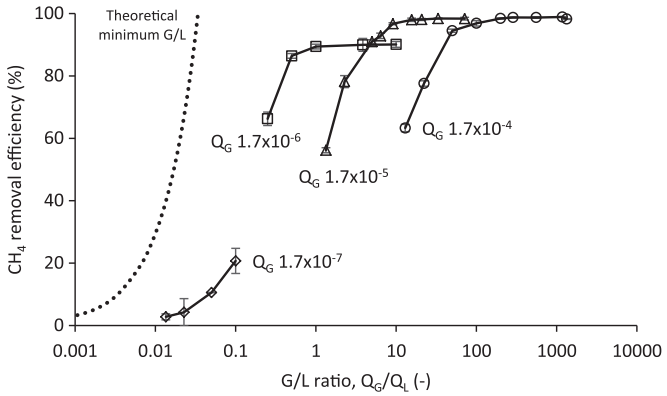

Fig. 3. Experimental CH_4 removal efficiencies at respective values of G/L ratio versus projected removal efficiencies at the 'theoretical minimum G/L'.

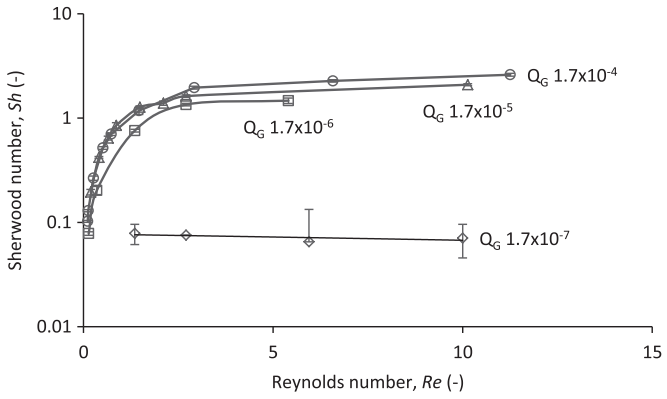

Fig. 4. Experimental CH_4 mass transfer as Sherwood number (Sh) versus Reynolds number (Re) in the liquid for several fixed values of Q_G (1.7×10^{-7}–1.7×10^{-4} $m^3\,s^{-1}$).

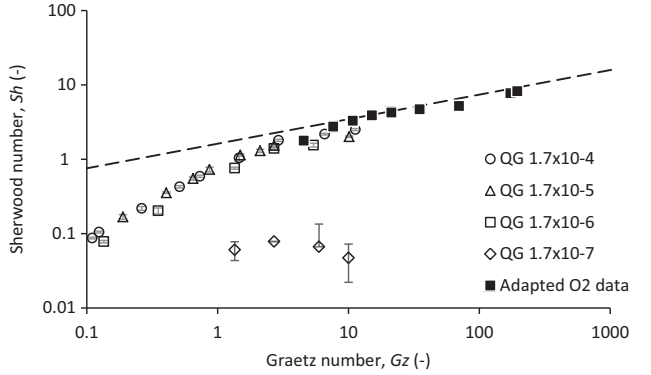

Fig. 5. Comparison of CH_4 mass transfer (present study) with data adapted for O_2 degas in a micro-porous HFMC (black filled shapes, adapted from Tai et al., 1994 [17]) and the Graetz–Lévèque solution (dashed line).

of mass transfer to the rate of diffusive mass transport (Fig. 4). Liquid phase Re ranged from 0.1 to 11 corresponding to entrance lengths (L_e) of between 1.1×10^{-6} m and 1.2×10^{-4} m ($(L_e = 0.05 Re_{liquid} d)$ which suggest entrance effects to reside in only a small fraction of the initial fibre length (L, 0.113 m). The Sh data increased from around 0.1–2.5 as Reynolds number in the liquid phase increased from 0.1 up to 11 (for fixed Q_G from 1.7×10^{-4} to 1.7×10^{-6} m^3 s^{-1}), which illustrated the dependency of mass transfer upon liquid velocity. However, at the lowest Q_G tested (1.67×10^{-7} $m^3\,s^{-1}$), mass transfer was independent of Re_{liquid}, remaining relatively constant across the hydrodynamic boundary conditions tested (Re_{liquid}, 2–11). The Graetz-Lévèque analytical solution, which provides an approximate solution for tube side

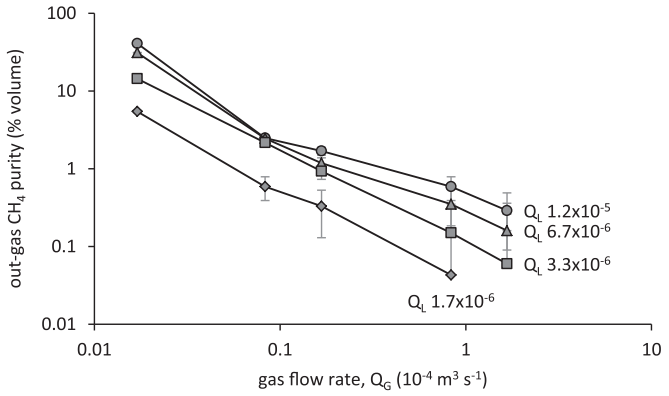

Fig. 6. Impact of Q_G (1.7×10^{-6}–1.7×10^{-4} $m^3\,s^{-1}$) upon out-gas CH_4 purity for fixed values of Q_L.

mass transfer, was compared to experimental Sh data (Fig. 5). Whilst the solution is generally only valid for $Gz > 20$, the solution provided reasonable description of experimental data at Gz numbers exceeding 10 as has been observed previously [25].

3.3. Methane concentration in the recovered gas phase

Methane purity within the recovered gas phase was investigated by varying Q_G (1.7×10^{-6}–1.7×10^{-4} $m^3\,s^{-1}$) for several fixed values of Q_L (1.7×10^{-6}–1.2×10^{-5} $m^3\,s^{-1}$) (Fig. 6). In general, for a fixed Q_L, the highest gas phase methane purity was observed at the lowest Q_G used. Furthermore, at low gas flow rates, the methane purity was further enhanced at higher Q_L. Consequently, the highest gas phase methane concentration was recorded when hydrodynamic conditions were fixed to the highest Q_L and lowest Q_G which corresponds to a low G/L ratio (Fig. 7). Interestingly, mass balance of the liquid phase dissolved methane removal data generally under-predicts the gas-phase CH_4 concentration (dashed line), with under-prediction of gas-side methane purity being particularly evident at the lower G/L range.

4. Discussion

The significant finding in this study was that dissolved methane could be recovered into the gas phase in sufficient concentration for reuse. To illustrate, the sweep gas comprised a methane concentration within the lower and upper flammable limits (5–15%), and at the lowest G/L ratios examined, the recovered gas-phase exceeded the upper flammable limit which

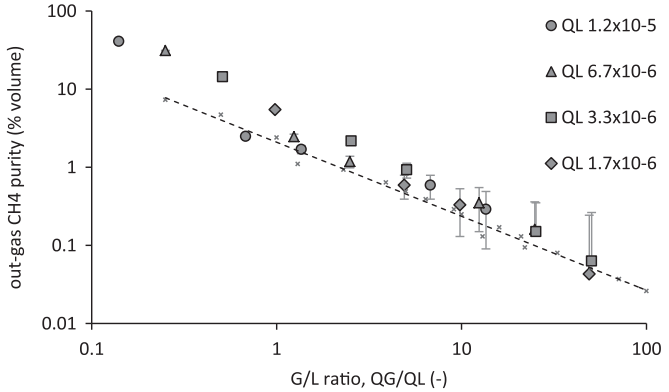

Fig. 7. Impact of Q_G (1.7×10^{-6}–1.7×10^{-4} $m^3\,s^{-1}$) upon out-gas CH_4 purity for fixed values of Q_L. Also presented is the estimated CH_4 purity based on mass balance of the dissolved methane removal data (dashed line).

demonstrates that is practically suitable for use in modern micro-turbines applied to electricity production [3]. Methane purity was enhanced in the gas phase through two primary mechanisms: (i) an increase in liquid velocity which improved dissolved methane mass transfer into the gas phase; and (ii) a reduction in gas flow which lowered dilution from the receiving gas phase. Gas phase methane purity can therefore be best enhanced through combination of both mechanisms, which was evidenced in this study through a reduction in the G/L ratio (Fig. 7). Interestingly, the measured methane purity was higher than estimated based on mass balance of the recovered methane into the receiving nitrogen sweep-gas and was exacerbated at low G/L ratios (dashed line, Fig. 7). Ahmed et al. used composite hollow fibre membranes to provide bubbleless aeration into water by supplying pure oxygen in the fibre lumen [19]. The authors described how dissolved gases such as nitrogen already present in the receiving water diffused back into the gas phase within the lumen due to a high nitrogen concentration gradient between the initially pure oxygen gas phase and the initially nitrogen saturated liquid phase. This counter-diffusion of nitrogen in to the gas phase proceeded until equilibrium was reached between the liquid and gas phases. In this study, the reverse of this mechanism is plausible since oxygen and methane share similar transport properties in water. The sweep gas used was initially 100% nitrogen whilst the initial water phase was saturated by CH_4 and CO_2 (i.e. zero dissolved nitrogen), creating a sizeable nitrogen concentration gradient between liquid and gas when interfaced by the membrane. Consequently it is asserted that the higher than expected CH_4 concentration in the final gas phase in this study can be explained by this nitrogen concentration gradient, which promoted the counter-diffusion of nitrogen from sweep gas into the water phase and subsequently enhanced CH_4 purity in the residual gas phase.

Dissolved methane removal efficiency of greater than 97% was demonstrated with the microporous HFMC. In a recent study, Cookney et al. [1] compared mass transfer coefficients estimated from dissolved methane recovery experiments with an analogue and an anaerobic MBR permeate and identified close parity between the two fluids, which evidences the potential for data translation into real wastewater application [1]. Whilst for a fixed gas flow rate, an increase in liquid velocity decreased removal efficiency, a simultaneous increase in mass transfer was observed. Similar behaviour was reported by Heile et al. during the absorption of CO_2 with a HFMC and can be ascribed to the higher concentration gradient that was sustained at the liquid-membrane interface when operated at the higher V_L [9]. Whilst this behaviour is indicative of liquid phase controlled mass transfer, a decrease in gas flow rate from 1.67×10^{-4} to 1.67×10^{-6} $m^3 s^{-1}$ at a fixed liquid flow rate diminished mass transfer by 22% (Table 1); and as gas flow rate was reduced to the lowest flow rate tested (Q_G 1.7×10^{-7} $m^3 s^{-1}$), this effect was exacerbated and *Sh* became independent of Re_{liquid} (Fig. 4). Cookney et al. suggested that dissolved methane mass transfer is non-limited when sweep gas-flow rate is in excess of the theoretical $G/L_{minimum}$ [4]. However, it is asserted that the reduction in mass transfer observed in this study following a reduction in gas-flow rate is due to the onset of gas phase controlled mass transfer and was identified at G/L considerably higher than the theoretical $G/L_{minimum}$. The early onset of gas-phase control can be attributed to poor shell-side dispersion caused by the relatively high HFMC packing density used (θ 0.37). Such behaviour was identified by Yang and Cussler during the desorption of oxygen from water [18]. Zheng et al. demonstrated mal-distribution of shell-side flow through modelling when θ exceeded 0.3 whereas other authors have evidenced strong data correlation at lower packing factions between 0.26 and 0.03 [20]. Use of a lower packing fraction, or addition of shell-side baffling such as that employed within full-scale HFMC modules to ameliorate dispersion limitations [21], should enable operation closer to the minimum G/L ratio, benefitting both mass transfer and gas-side methane purity (Table 1).

Table 1
Impact of reduction in sweep gas flow on liquid phase mass transfer coefficient.

Gas flow rate, Q_G ($\times 10^{-5}$ $m^3 s^{-1}$)	Liquid flow rate, Q_L ($\times 10^{-5}$ $m^3 s^{-1}$)	Liquid mass transfer coefficient, K_L ($\times 10^{-5}$ $m s^{-1}$)
16.7	3.33	1.54
1.67	3.33	1.31
0.167	3.33	1.20

Table 2
Estimation of the dissolved methane recovery required to achieve carbon neutrality.

Parameter	Value		Estimate	
Density of methane[a]	670	g m^{-3}		
Energy density of methane[a]	10	kWh m^{-3}		
Electrical conversion efficiency[a]	40	%		
Electrical energy recovered from 1 g CH_4			0.006	kWh g^{-1}
Grid elec. CO_2 footprint[a]	543	g kWh^{-1}		
GWP of CH_4[a]	23	gCO_2 gCH_4^{-1}		
Renewable electrical energy needed to offset 1 g fugitive CH_4			0.042	kWh g^{-1}
Example mass balance (25 gCH_4 m^{-3})				
88% CH_4 recovery in HFMC			0.132	kWh m^{-3}
12% CH_4 in effluent			0.126	kWh m^{-3}
Net difference			+0.006	*Carbon neutral*

[a] Values from literature (McAdam et al. [24]).

To achieve carbon neutrality, over 88% of the dissolved methane has to be recovered from the wastewater for reuse in energy production (Table 2). At high sweep gas flow rates (high G/L ratios) the dissolved methane removal efficiency demonstrated by the microporous HFMC exceeded this threshold within retention times of between 3.3 s and 22.9 s. However, the methane purity needed for reuse requires operation at low gas flow rates which restricted mass transfer and introduces a trade-off between the usability of the recovered gas phase and the dissolved methane removal efficiency of a single stage HFMC (Fig. 8). Vallieres and Favre suggested that vacuum may be more favourable when gas phase purity is important as vacuum obviates dilution [22]. Bandara et al. and Cookney et al. both used vacuum and were able to

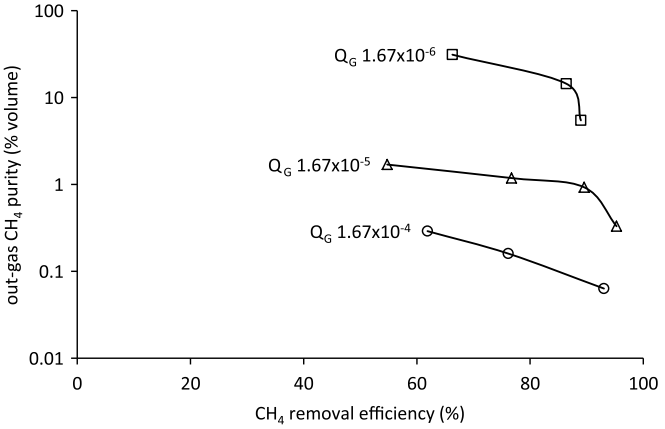

Fig. 8. Trade-off between removal efficiency and purity of recovered CH_4.

achieve a methane concentration of up to 27% in the recovered gas phase (Bandara et al.) with the authors indicating that higher concentrations were achievable [4,12]. However, low operating vacuum pressures are necessary to ensure that vacuum does not impose gas phase controlled mass transfer. To illustrate, Ito et al. achieved 17% dissolved oxygen removal at a vacuum pressure of 52 kPa which increased to 80% when vacuum was increased to 4 kPa [23]. This is analogous to the effective operating vacuum pressure reported by Cookney et al. for dissolved methane removal from wastewater which is energetically constraining and when applied to microporous HFMC, such vacuum pressures are also likely to promote pore wetting [4]. Importantly, in this study, a microporous HFMC operated in sweep-gas mode has been demonstrated to recover methane in usable form using only short residence times which establishes the practical viability of recovery. Both the treatment objective (i.e. greater than 88% removal efficiency) and the recovery of methane for reuse can be achieved under gas phase controlled conditions through placing HFMC in series which has been shown to remain economically viable despite the increase in pressure drop and necessary membrane area [1].

5. Conclusions

In this study, a micro-porous hollow fibre membrane contactor operated in sweep-gas mode has been shown to enable the recovery of dissolved methane at sufficient gas concentration to be reused in energy production. At high sweep-gas flow rates, up to 97% dissolved methane removal efficiency is achieved and mass transfer could be regarded as liquid phase controlled. Above 88% dissolved CH_4 recovery can be regarded as carbon neutral electrical generation (Table 2). Carbon neutrality is achieved when the fugitive emission of CH_4 (23 CO_2 equivalents [24]) to the atmosphere is sufficiently reduced (in this case by dissolved CH_4 recovery in the HFMC) that the CO_2 equivalents (CO_2 eq.) associated with grid electricity are fully offset by substitution for electricity generated by combustion of the renewable biogas. Methane composition in the recovered sweep-gas was primarily controlled by an increase in liquid velocity which improved dissolved methane mass transfer into the gas phase and a reduction in gas flow which lowered dilution from the receiving gas phase. However, as the gas-liquid ratio was lowered to improve gas-side methane purity, mass transfer became increasingly gas-phase controlled. Whilst the resultant reduction in removal efficiency can be compensated for by extending path length (i.e. more than one module in series), the gas-phase controlled conditions encountered in this study were also a product of poor shell-side dispersion rather than an approach toward the limiting theoretical gas-to-liquid ratio, which implies that further optimisation can be ascertained through membrane contactor design. Importantly, this study demonstrates that micro-porous hollow fibre membrane contactors provide a compact process for recovery of dissolved methane in sufficient concentration for re-use.

Acknowledgements

The authors would like to thank the Engineering and Physical Sciences Research Council (EPSRC, V/N: 08001923), Anglian Water, Northumbrian Water, Severn Trent Water and Yorkshire Water for their financial support. Enquiries for access to the data referred to in this article should be directed to: researchdata@cranfield.ac.uk.

References

[1] J. Cookney, A. Mcleod, V. Mathioudakis, P. Ncube, A. Soares, B. Jefferson, et al., Dissolved methane recovery from anaerobic effluents using hollow fibre membrane contactors, J. Membr. Sci. 502 (2016) 141–150, http://dx.doi.org/10.1016/j.memsci.2015.12.037.
[2] H.D. Robinson, M. Carville, The use of pilot-scale trials in the design and state of the art leachate treatment plants, in: Proceedings of Waste 2010 Conf., Stratford-Upon-Avon, 2010.
[3] Capstone, CR65 & CR65-ICHP MicroTurbine Renewable. ⟨http://www.regattasp.com/files/CR65&CR65-ICHP_Renewable_331039D.pdf⟩, 2010 (accessed 27.01.16).
[4] J. Cookney, E. Cartmell, B. Jefferson, E.J. McAdam, Recovery of methane from anaerobic process effluent using poly-di-methyl-siloxane membrane contactors, Water Sci. Technol. 65 (2012) 604–610, http://dx.doi.org/10.2166/wst.2012.897.
[5] D.A. Pittam, G. Pilcher, Measurements of heats of combustion by flame calorimetry: Part 8.-Methane, ethane, propane, n-butane and 2-methylpropane, J. Chem. Soc. Faraday Trans. 1 (68) (1972) 2224–2229, http://dx.doi.org/10.1039/f19726802224.
[6] M.R.J. Daelman, E.M. van Voorthuizen, U.G.J.M. van Dongen, E.I.P. Volcke, M.C. M. van Loosdrecht, Methane emission during municipal wastewater treatment, Water Res. 46 (2012) 3657–3670, http://dx.doi.org/10.1016/j.watres.2012.04.024.
[7] J.C. Crittenden, R.R. Trussell, D.W. Hand, K.J. Howe, G. Tchobanoglous, MWH'S Water Treat., http://dx.doi.org/10.1002/9781118131473.
[8] D.W. Hand, J.C. Crittenden, J.L. Gehin, B.W. Lykins Jr., Design and evaluation of an air-stripping tower for removing VOCs from groundwater, J. Am. Water Works Assoc. 78 (1986) 87–97.
[9] S. Heile, S. Rosenberger, A. Parker, B. Jefferson, E.J. McAdam, Establishing the suitability of symmetric ultrathin wall polydimethylsiloxane hollow-fibre membrane contactors for enhanced CO_2 separation during biogas upgrading, J. Membr. Sci. 452 (2014) 37–45, http://dx.doi.org/10.1016/j.memsci.2013.10.007.
[10] J. He, R.G. Arnold, A.E. Saez, E.A. Betterton, W.P. Ela, Removal of aqueous phase trichloroethylene using membrane air stripping contactors, J. Environ. Eng. 130 (2004) 1232–1241.
[11] T. a Cramer, D.W. Johnson, A. Urynowicz, Membrane gas transfer of methane and carbon dioxide in submerged coal deposits, Environ. Technol. 30 (2009) 11–20, http://dx.doi.org/10.1080/09593330802421425.
[12] Wasala M.K.R.T.W. Bandara, Hisashi Satoh, Manabu Sasakawa, Yoshihito Nakahara, Masahiro Takahashi, Satoshi Okabe, Removal of residual dissolved methane gas in an upflow anaerobic sludge blanket reactor treating low-strength wastewater at low temperature with degassing membrane, Water Res. 45 (2011) 3533–3540, http://dx.doi.org/10.1016/j.watres.2011.04.030.
[13] A. Alkhudhiri, N. Darwish, N. Hilal, Membrane distillation: a comprehensive review, Desalination. 287 (2012) 2–18, http://dx.doi.org/10.1016/j.desal.2011.08.027.
[14] D. Mackay, W.Y. Shiu, A critical review of Henry's law constants for chemicals of environmental interest, J. Phys. Chem. Ref. Data 10 (1981) 1175, http://dx.doi.org/10.1063/1.555654.
[15] P.A. Witherspoon, D.N. Saraf, Diffusion of methane, ethane, propane, and n-butane in water from 25° to 43°, J. Phys. Chem. 69 (1965) 3752–3755, http://dx.doi.org/10.1021/j100895a017.
[16] M.C. Alberto, J.R. Arah, H. Neue, R. Wassmann, R. Lantin, J. Aduna, et al., A sampling technique for the determination of dissolved methane in soil solution, Chemosphere Glob. Change Sci. 2 (2000) 57–63, http://dx.doi.org/10.1016/S1465-9972(99)00044-6.
[17] M.S.L. Tai, I. Chua, K. Li, W.J. Ng, W.K. Teo, Removal of dissolved oxygen in ultrapure water production using microporous membrane modules, J. Membr. Sci. 87 (1–2) (1994) 99–105, http://dx.doi.org/10.1016/0376-7388(93)E0086-S.
[18] M.-C. Yang, E.L. Cussler, Designing hollow-fiber contactors, AIChE J. 32 (1986) 1910–1916.
[19] T. Ahmed, M.J. Semmens, The use of independently sealed microporous hollow fiber membranes for oxygenation of water: model development, J. Membr. Sci. 69 (1992) 11–20, http://dx.doi.org/10.1016/0376-7388(92)80163-E.
[20] J. Zheng, Y. Xu, Z. Xu, Flow distribution in a randomly packed hollow fiber membrane module, J. Membr. Sci. 211 (2003) 263–269, http://dx.doi.org/10.1016/S0376-7388(02)00426-X.
[21] A. Gabelman, S. Hwang, Hollow fiber membrane contactors, J. Membr. Sci. 159 (1999) 61–106, http://dx.doi.org/10.1016/S0376-7388(99)00040-X.
[22] C. Vallieres, E. Favre, Vacuum versus sweeping gas operation for binary mixtures separation by dense membrane processes, J. Membr. Sci. 244 (2004) 17–23, http://dx.doi.org/10.1016/j.memsci.2004.04.023.
[23] A. Ito, K. Yamagiwa, M. Tamura, M. Furusawa, Removal of dissolved oxygen using non-porous hollow-fiber membranes, J. Membr. Sci. 145 (1998) 111–117, http://dx.doi.org/10.1016/S0376-7388(98)00068-4.
[24] E.J. McAdam, D. Lüffler, N. Martin-Garcia, A.L. Eusebi, J.N. Lester, B. Jefferson, Integrating anaerobic processes into wastewater treatment, Water Sci. Technol. 63 (2011) 1459–1466, http://dx.doi.org/10.2166/wst.2011.378.
[25] S.R. Wickramasinghe, M.J. Semmens, E.L. Cussler, Mass transfer in various hollow fiber geometries, J. Membr. Sci. 69 (1992) 235–250.